# Combining cw-seeding with highly nonlinear fibers in a broadly tunable femtosecond optical parametric amplifier at 42 MHz

**Tobias Steinle,* Stefan Kedenburg, Andy Steinmann, and Harald Giessen**

*4th Physics Institute and Research Center SCOPE, University of Stuttgart, 70550 Stuttgart, Germany*
**Corresponding author: t.steinle@pi4.uni-stuttgart.de*

Received March 25, 2014; accepted April 25, 2014;
posted May 13, 2014 (Doc. ID 208819); published August 13, 2014

We report on a precisely tunable and highly stable femtosecond oscillator-pumped optical parametric amplifier at a 41.7 MHz repetition rate for spectroscopic applications. A novel concept based on cw-seeding of a first amplification stage with subsequent spectral broadening and shaping, followed by two further amplification stages, allows for precise sub-nanometer and gap-free tuning from 1.35 to 1.75 μm and 2.55 to 4.5 μm. Excellent spectral stability is demonstrated with deviations of less than 0.008% rms central wavelength and 1.6% rms bandwidth over 1 h. Spectral shaping of the seed pulse allows precise adjustment of both the bandwidth and the pulse duration over a broad range at a given central wavelength. Transform-limited pulses nearly as short as 107 fs are achieved. More than half a Watt of average power in the near- and more than 200 mW in the mid-infrared with power fluctuations less than 0.6% rms over 1 h provide an excellent basis for spectroscopic experiments. The pulse-to-pulse power fluctuations are as small as 1.8%. Further, we demonstrate for the first time, to the best of our knowledge, that by using hollow-core capillaries with highly nonlinear liquids as a host medium for self-phase modulation, the signal tuning range can be extended and covers the region from 1.4 μm up to the point of degeneracy at 2.07 μm. Hence, the idler covers 2.07 to 4.0 μm. 

*OCIS codes:* (140.7090) Ultrafast lasers; (190.4410) Nonlinear optics, parametric processes; (190.4970) Parametric oscillators and amplifiers; (190.7110) Ultrafast nonlinear optics; (320.7140) Ultrafast processes in fibers.
http://dx.doi.org/10.1364/OL.39.004851

The generation of coherent multiwavelength near-infrared laser radiation is essential for future breakthroughs in spectroscopic applications. As an example, both coherent anti-Stokes and stimulated Raman scattering spectroscopy require tunable low-noise ultrafast laser sources [1]. The approaches to generate synchronized pump and Stokes beams are electronically and optically synchronized solid-state lasers [2], combined fiber amplifier systems, where pulses from a master oscillator are spectrally broadened in highly nonlinear fibers and then amplified by Yb-, Er-, or Tm-fiber amplifiers [3], synchronously pumped optical parametric oscillators (OPOs) [4,5], and, at low repetition rates, optical parametric amplifiers (OPAs) [6,7].

These parametric sources simultaneously generate mid-infrared wavelengths, which are highly important to extend the wavelength range into the molecular fingerprint region from 2 to 12 μm [8]. In this spectral region, various applications such as medical diagnostics, surgery, imaging, remote sensing, and chemical detection generate a strong demand for powerful and reliable laser sources. The main advantage of having parametric sources beside the synchronized outputs is their ultrabroad tunability of several micrometers [9,10] in comparison with mid-infrared laser systems that are limited to the gain bandwidth of the laser medium [11,12].

A major disadvantage of the OPO systems is the requirement for active cavity stabilization to maintain the synchronous operation and to stabilize power and wavelength [13]. It is also known that injection seeding with a cw laser improves the wavelength stability [14] of the OPOs, while for OPAs cw-seeding has been shown to lead to nearly transform limited pulses [15]. Typical OPA systems are pumped by regenerative amplifiers with a repetition rate of several kilohertz, and therefore suffer from low average power obtained from large and complex setups.

In this Letter, we demonstrate a compact broadly tunable oscillator-pumped OPA at a 41.7 MHz repetition rate seeded by a broad continuum from a tapered fiber pumped by a cw-seeded OPA, which is operated in the center of the system tuning range. This fiber pump wavelength is shifted spectrally with respect to the oscillator and allows employment of highly nonlinear liquids such as $CS_2$ in hollow-core capillaries as viable alternative to tapered or photonic crystal fibers, which we demonstrate here for the first time to the best of our knowledge.

Our cw-seeded OPA involves a minimum amount of optical components, benefits from easy alignment, and represents a long-term stable and reliable femtosecond source at any desired wavelength, only limited by the transmission of the nonlinear crystal. The main advantage is that no spectral broadening of the pump by third-order parametric processes is required, since the conversion is easily obtained by a single pass in a nonlinear crystal at the presence of a cw-seed. Hence, there are very low timing-jitter effects, and since a solid-state oscillator is employed as the pump source, low high-frequency noise can be achieved in comparison with fiber amplifier systems [16].

Pumping the nonlinear fiber in the center of the OPA tuning range is superior to systems where the supercontinuum and the OPA are pumped at the same wavelength since, in the latter case, very broad supercontinua are required [9]. For these, it is often difficult to maintain the coherence, since especially at a high repetition rate, one needs to pump in the anomalous dispersion regime to reach large bandwidths [17]. Both approaches, the tapered fiber and the highly nonlinear liquid-filled fiber,

 

are operated mainly in the normal dispersion regime or very close to the zero dispersion wavelength (ZDW).

The system is pumped by a Yb:KGW solid-state oscillator capable of delivering 7.4 W at 41.7 MHz and 1033 nm with a pulse duration of 450 fs [18]. This laser is directly followed by a cw-seeded parametric conversion stage as shown in Fig. 1. A 10 mm long MgO:PPLN crystal is used to generate up to 300 mW at 1540 nm with a pulse duration of 250 fs by using 1.5 W of pump power. The cw-seed is provided by a Fabry–Perot laser diode with 20 mW power at 1540 nm. The pulses with 12.5 nm bandwidth are slightly chirped due to the large crystal length. This seed is then spectrally broadened in a nonlinear fiber. Both a thin tapered fiber [19] with 1.25 μm waist diameter and 8.5 cm waist length, and a $CS_2$-filled capillary with a 2 μm core diameter and 24 cm fiber length are employed for spectral broadening. While the easy handling of the tapered fiber provides more stable and higher output power, the huge nonlinearity of the liquid-filled fiber provides extremely broad seed spectra [20,21]. The generated broadband spectra are spectrally shaped using a prism sequence and a mechanical slit. This ensures that only a narrow linewidth seed is used for the subsequent power amplification stages. For the first parametric amplification stage, the spectrally shaped seed is amplified to a power level of approximately 50 mW at a pump power of 1.4 W in a 5 mm long MgO:PPLN crystal with poling periods from 26.5 to 31.5 μm. The second stage uses an identical 3 mm long crystal and is pumped with 2.5 W power, amplifying the signal to the Watt level. As shown in [22], this two-stage scheme ensures that relative timing-jitters between seed and pump source, which can arise from soliton formation in nonlinear fibers, are eliminated. Finally, the pulses are temporally compressed in a prism compressor behind the second amplification stage.

For the tapered fiber case, which we will discuss first, the generated seed spectrum is shown in Fig. 2(c). The pump pulses at 1540 nm are very close to the ZDW of the tapered fiber of 1590 nm. Therefore, the spectrum shows a mixture of a single solitonic peak at 1600 nm and a broad plateau ranging from 1350 to 1750 nm which originates mainly from the self-phase-modulation, leading to good coherence of the supercontinuum [17]. The spectral filter makes it possible to cut out a narrow region of this spectrum with adjustable linewidth down to 15 nm

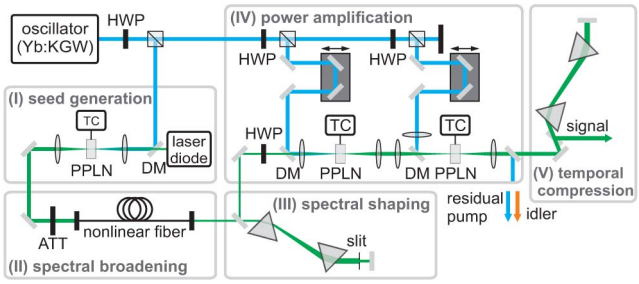


Fig. 1. Experimental setup consisting of (I) a cw-seeded parametric amplification stage, (II) a thin tapered or liquid-filled fiber, (III) a prism monochromator, (IV) a parametric power amplifier, and (V) a prism compressor sequence. HWP, half-wave plate; DM, dichroic mirror; ATT, variable attenuator; TC, temperature controller; and PPLN, periodically poled lithium niobate crystal.

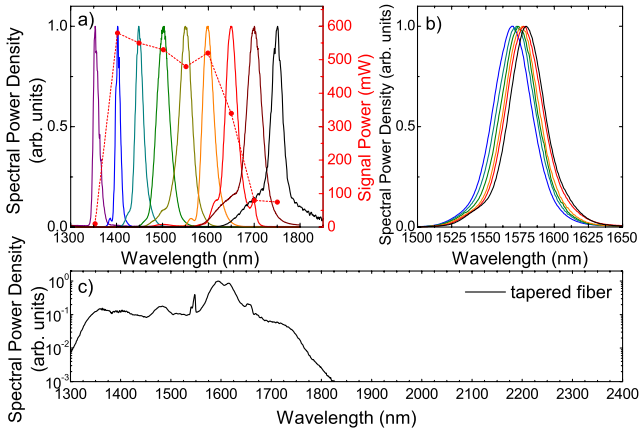


Fig. 2. (a) Signal tuning spectra over the whole tuning range from 1350 to 1750 nm central wavelength and (b) fine tuning in steps of 2 nm around 1575 nm using the spatial filter. The peak at 1750 nm shows a pedestal which results from upcoming optical parametric generation. (c) For wavelengths shorter than 1750 nm, the optical parametric generation is efficiently suppressed by the seed.

(FWHM), which is then used as a seed for the first parametric amplification stage. The tuning spectra shown in Fig. 2(a) demonstrate continuous signal tunability from 1350 to 1750 nm. This matches well with the seed bandwidth.

The signal power level is around 500 mW in the range from 1400 to 1600 nm and then drops because of the decreasing seed power down to 100 mW at 1750 nm. Signal power up to 1 W is obtained if the bandwidth is not limited by the spectral filter, but this also causes spectral and power instabilities over time. The precisely adjustable seed also allows for precise gap-free tuning of the signal wavelength as demonstrated in Fig. 2(b).

By tuning the seed bandwidth with the spatial filter, the signal bandwidth can be influenced, which is depicted in Fig. 3. At a central wavelength of 1575 nm, the bandwidth can be varied continuously from 22 to 40 nm. Since this requires a broad parametric gain bandwidth [23], the achievable bandwidths are wavelength

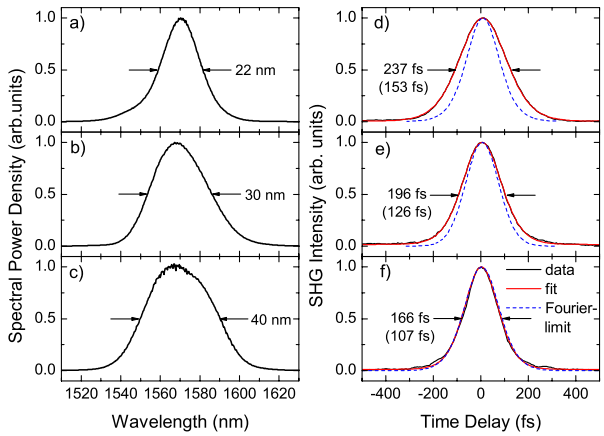


Fig. 3. Variation of bandwidth by shaping the seed spectrum (a)–(c) from 22 to 40 nm at 1575 nm central wavelength and (d)–(f) corresponding autocorrelations after a prism compressor. Before compression, the pulse duration is typically on the order of 180 fs. The given values are autocorrelation FWHM and pulse duration assuming $\mathrm{sech}^2$ pulses (embraced value).

dependent and increase for higher wavelengths. Figure 3 further demonstrates that, after the prism compressor, almost transform-limited pulses are obtained with pulse durations as low as 107 fs and a typical time–bandwidth product of 0.4–0.5. Compression is particularly useful for pulses with high spectral bandwidth, since the pulse duration behind the second conversion stage remains approximately constant at 180 fs, because of the duration of the pump pulse. A pulse duration of less than 150 fs after compression can be reproduced in the signal tuning range from 1450 nm to at least 1600 nm, which is the upper limit of our autocorrelator. For shorter wavelengths, the narrow parametric gain bandwidth leads to longer pulses of about 200 fs.

The system further shows excellent temporal stability on both the microsecond timescale and over several hours. Figure 4 proves that, the pulse-to-pulse power fluctuations are within 1.8% rms which is because of the combination of a coherent seed and a two-stage power amplifier. Further, the stability of the average power is as good as 0.6% rms over 1 h. Figure 4(c) demonstrates that the central wavelength deviates less than 0.008% rms over 1 h, while the bandwidth varies by 1.6% rms over the same timespan.

Because of the wavelength-dependence of both the parametric gain and the gain bandwidth, the performance also changes with wavelength. Increasing the wavelength will result in lower performance, while decreasing the wavelength will, in general lead to better performance. However, there is optimum performance close to 1540 nm because of the fact that there is less broadening of the seed required and therefore both the seed spectral power density and seed stability increase.

Altogether, the single-pass scheme makes this system very robust to environmental conditions, while the high parametric gain in the power amplifier ensures inherently stable operation. Unlike comparable OPOs, there is neither synchronous pumping nor active stabilization required.

By replacing the tapered silica fiber with a liquid-filled capillary fiber with a 2 μm core of $CS_2$ and a total length of 24 cm, the tuning range of the system can be extended from 1400 to 2065 nm, as shown in Fig. 5. The generated idler, which is not further investigated here, ranges from 2.07 to 4.0 μm. The very broad seed spectrum [cf. Fig. 5(b)] from the highly nonlinear $CS_2$-filled capillary ranges from 1400 to 2125 nm. The broadening

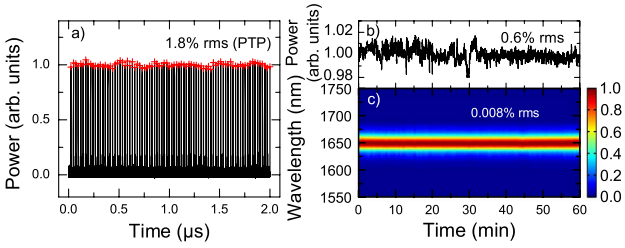


Fig. 4. Pulse-to-pulse stability over 2 μs (a) and temporal stability of average power over 1 h measured with 10 Hz bandwidth (b) at 1600 nm. Spectral stability close to the edge of the tuning range at 1650 nm over 1 h (c). The performance will increase if the wavelength is chosen closer to the cw-seed wavelength of 1540 nm.

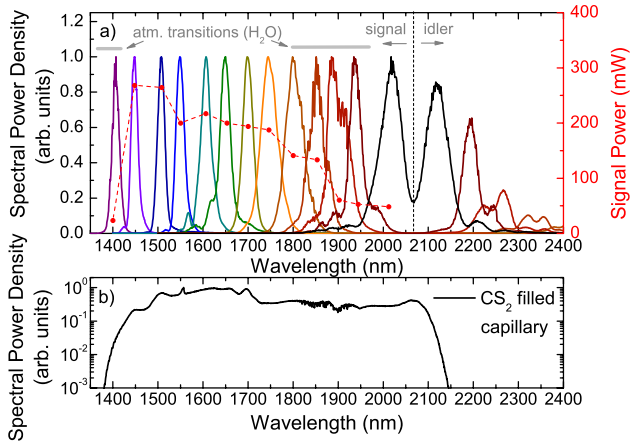


Fig. 5. Signal spectra showing a tuning range starting at 1400 nm. (a) The signal can be tuned up to 2065 nm, where the signal and idler are degenerate. The measured power for signal wavelengths higher than 1750 nm includes a share of the idler, which is also visible in the spectrum. (b) Seed spectrum emerging from a 24 cm long $CS_2$-filled capillary with 2.0 μm core diameter. The atmospheric transition lines of water vapor are visible in the spectra from 1800 to 1950 nm.

takes place in the normal dispersion regime under strong influence of self-phase modulation and retarded response effects [20]. The flat and smooth spectrum facilitates the spectral shaping of the seed pulses. Note that both the seed and the signal spectra are taken with a grating spectrometer in free-space configuration, so that a distance of 1–4 m in air has been passed, which explains the absorption lines due to water vapor in the 1800 to 1950 nm region.

The maximum OPA signal power is lower compared to the tapered fiber case, since the spectral power density obtained from the liquid-filled fiber is significantly lower. While the spectrum covers a bandwidth of 900 nm, the actual output power is about 20–30 mW compared to up to 50 mW from the tapered fiber. Further, the allowed delay between seed and pump pulses of the first stage indicates that the pulses from the liquid-filled capillary are strongly chirped and last several picoseconds. All in all, the seed peak power is lower compared to the tapered fiber by at least a factor of four after the spectral shaper, which explains the lower signal power. The limiting factor for the transmitted power is mainly the rather low coupling efficiency to the 2 μm core for the liquid-filled fiber. Because of the part of the seed beam that did not transmit, the fiber input end heats up and evaporates the liquid, hence destroying the fiber input coupling and limiting the fiber input power. In contrast to the silica fiber which is used to couple into the tapered fiber, the liquid-filled fiber turns out to be sensitive on environmental conditions, and the system has to be realigned over time. For a time frame of several minutes, the device showed good performance without realignment. Technical engineering such as sealing the liquid-filled capillary by splicing silica fibers at both ends could improve the performance [24].

To conclude, we have demonstrated an optical parametric amplification scheme, which is able to cover a tuning range of 1.35–4.5 μm with adjustable spectral bandwidth in the range of 20–40 nm. The nearly

transform-limited femtosecond pulses from 100 to 200 fs show significant pulse shortening compared to the pulse duration of the pump source of 450 fs. With a tapered fiber for spectral broadening, the system exhibits excellent short- and long-term temporal and spectral stability without the need for active stabilization mechanisms. By employing a $CS_2$-filled capillary instead of a tapered fiber, the tuning range could be extended significantly.

We acknowledge financial support from Baden-Württemberg-Stiftung (PROTEINSENS), Deutsche Forschungsgemeinschaft (SPP1391), the European Research Council (COMPLEXPLAS), Zeiss-Stiftung, and Alexander von Humboldt Stiftung. This work was supported by the German Research Foundation (DFG) within the funding program Open Access Publishing.

**References**

1. R. Selm, M. Winterhalder, A. Zumbusch, G. Krauss, T. Hanke, A. Sell, and A. Leitenstorfer, Opt. Lett. **35**, 3282 (2010).
2. D. Yoshitomi, Y. Kobayashi, M. Kakehata, H. Takada, and K. Torizuka, Opt. Express **14**, 6359 (2006).
3. S. Kumkar, G. Krauss, M. Wunram, D. Fehrenbacher, U. Demirbas, D. Brida, and A. Leitenstorfer, Opt. Lett. **37**, 554 (2012).
4. D. C. Edelstein, E. S. Wachman, and C. L. Tang, Appl. Phys. Lett. **54**, 1728 (1989).
5. T. I. Ferreiro, J. Sun, and D. T. Reid, Opt. Express **19**, 24159 (2011).
6. M. Greve, B. Bodermann, H. R. Telle, P. Baum, and E. Riedle, Appl. Phys. B **81**, 875 (2005).
7. A. Killi, A. Steinmann, G. Palmer, U. Morgner, H. Bartelt, and J. Kobelke, Opt. Lett. **31**, 125 (2006).
8. A. Schliesser, N. Picqué, and T. W. Hänsch, Nat. Photonics **6**, 440 (2012).
9. J. Krauth, A. Steinmann, R. Hegenbarth, M. Conforti, and H. Giessen, Opt. Express **21**, 11516 (2013).
10. S. Marzenell, R. Beigang, and R. Wallenstein, Appl. Phys. B **69**, 423 (1999).
11. N. Tolstik, E. Sorokin, and I. T. Sorokina, Opt. Lett. **38**, 299 (2013).
12. I. T. Sorokina, E. Sorokin, S. Mirov, V. Fedorov, V. Badikov, V. Panyutin, and K. Schaffers, Opt. Lett. **27**, 1040 (2002).
13. N. Coluccelli, H. Fonnum, M. Haakestad, A. Gambetta, D. Gatti, M. Marangoni, P. Laporta, and G. Galzerano, Opt. Express **20**, 22042 (2012).
14. J. E. Bjorkholm and H. G. Danielmeyer, Appl. Phys. Lett. **15**, 171 (1969).
15. S. Hädrich, T. Gottschall, J. Rothhardt, J. Limpert, and A. Tünnermann, Opt. Express **18**, 3158 (2010).
16. K. Nose, Y. Ozeki, T. Kishi, K. Sumimura, N. Nishizawa, K. Fukui, Y. Kanematsu, and K. Itoh, Opt. Express **20**, 13958 (2012).
17. G. Genty, S. Coen, and J. M. Dudley, J. Opt. Soc. Am. B **24**, 1771 (2007).
18. A. Steinmann, B. Metzger, R. Hegenbarth, and H. Giessen, in *Conference on Lasers and Electro-Optics*, OSA Technical Digest (CD) (Optical Society of America, 2011), paper CThAA5.
19. J. Teipel, K. Franke, D. Türke, F. Warken, D. Meiser, M. Leuschner, and H. Giessen, Appl. Phys. B **77**, 245 (2003).
20. S. Kedenburg, A. Steinmann, R. Hegenbarth, T. Steinle, and H. Giessen, "Nonlinear refractive indices of nonlinear liquids: wavelength dependence and influence of retarded response," Appl. Phys. B, doi: 10.1007/s00340-014-5833-y (2014).
21. K. Kieu, L. Schneebeli, R. A. Norwood, and N. Peyghambarian, Opt. Express **20**, 8148 (2012).
22. T. Steinle, A. Steinmann, R. Hegenbarth, and H. Giessen, Opt. Express **22**, 9567 (2014).
23. G. Cerullo and S. De Silvestri, Rev. Sci. Instrum. **74**, 1 (2003).
24. L. Xiao, N. V. Wheeler, N. Healy, and A. C. Peacock, Opt. Express **21**, 28751 (2013).